

# Optical controlling reveals time-dependent roles for adult-born dentate granule cells

Yan Gu<sup>1</sup>, Maithe Arruda-Carvalho<sup>2,3</sup>, Jia Wang<sup>1</sup>, Stephen R Janoschka<sup>1,4</sup>, Sheena A Josselyn<sup>2,3,5</sup>, Paul W Frankland<sup>2,3,5</sup> & Shaoyu Ge<sup>1,4</sup>

Accumulating evidence suggests that global depletion of adult hippocampal neurogenesis influences its function and that the timing of the depletion affects the deficits. However, the behavioral roles of adult-born neurons during their establishment of projections to CA3 pyramidal neurons remain largely unknown. We used a combination of retroviral and optogenetic approaches to birth date and reversibly control a group of adult-born neurons in adult mice. Adult-born neurons formed functional synapses on CA3 pyramidal neurons as early as 2 weeks after birth, and this projection to the CA3 area became stable by 4 weeks in age. Newborn neurons at this age were more plastic than neurons at other stages. Notably, we found that reversibly silencing this cohort of ~4-week-old cells after training, but not cells of other ages, substantially disrupted retrieval of hippocampal memory. Our results identify a restricted time window for adult-born neurons essential in hippocampal memory retrieval.

The adult hippocampus continues to give rise to several thousand new dentate granule cells each day<sup>1–3</sup>. Accumulating evidence from studies using global perturbation or ablation of adult hippocampal neurogenesis has revealed deficits in some forms of hippocampal memory in rodents<sup>4–9</sup>. As the morphological and physiological phenotypes of adult-born cells change markedly as they mature, they may have distinct roles at different stages following integration into hippocampal circuits. Accordingly, although traditional manipulations of adult neurogenesis may disrupt hippocampal memory function, it is not clear whether the observed memory deficits are a result of a global disruption of neurogenesis.

Emerging evidence has shown that surviving adult-born dentate granule cells (DGCs) extend dendrites and receive functional input from the existing neural circuits as early as 2 weeks after birth<sup>10–14</sup>. In contrast with the many studies on input synapses, little is known about the establishment of functional projection of adult-born DGCs to the hippocampal trisynaptic circuit. Although massive effort has been put into determining output circuit formation of adult-born neurons, most evidence is from anatomical examinations showing that young newborn DGCs gradually extend axonal fibers into the CA3 area. Terminals of these axons form bouton-like structures similar to those of mature granule cells 2–3 weeks after birth<sup>15–18</sup>. A recent study found that mature newborn neurons exhibit synaptic responses in the CA3 area<sup>16</sup>. However, the precise timing for functional output synapse formation and maturation remains unknown.

Input (dendritic) synapses of adult-born neurons show enhanced plasticity between 4–6 weeks after birth compared with other stages<sup>19</sup>, at which point they exhibit heightened intrinsic excitability and lower activation threshold<sup>13,20</sup>. This coincides with the timing when

newborn neurons are recruited into adult neural circuits mediating behavior<sup>21–23</sup>. These findings suggest that a cohort of young adult-born neurons of similar age may form a hypersensitive unit that preferentially responds to stimuli during hippocampal memory formation. A related question is whether output synapses, if formed and functional, also exhibit heightened plasticity around the same time.

Combining retroviral birth-dating and gene delivery<sup>10,11</sup> with optogenetic stimulation<sup>24</sup>, we examined the behavioral roles of adult-born neurons during their output circuit development. We found that adult-born DGCs established functional synapses with CA3 pyramidal neurons as early as 2 weeks after birth and synaptic responses became stable by ~4 weeks of age. Fully established output synapses of adult-born neurons exhibited enhanced plasticity at ~4 weeks after birth. Notably, optogenetic silencing of a cohort of 4-week-old, but not 2- or 8-week-old, newborn neurons substantially affected the retrieval of hippocampal-dependent memory following the completion of training, suggesting that 4-week-old new neurons have a privileged role in hippocampal memory function. These data characterize the development of output circuit function for adult-born DGCs, revealing a precise time window in which newborn neurons exhibit enhanced plasticity at CA3 synapses and are critical for processing hippocampal memories.

## RESULTS

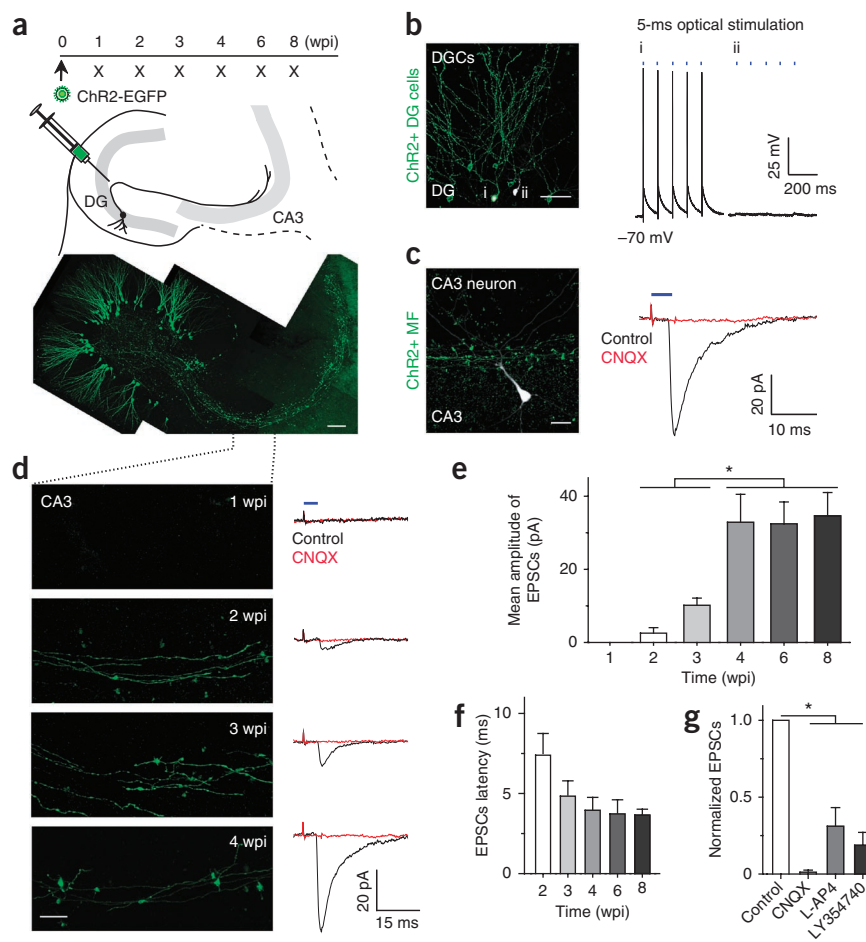
### Establishment of output synapses of adult-born neurons

To examine the role of adult-born neurons in hippocampal function during their circuit integration, we first determined the timing for newborn neurons to establish functional projections to CA3 pyramidal neurons. We used an optogenetic method to excite a group of

<sup>1</sup>Department of Neurobiology and Behavior, SUNY at Stony Brook, Stony Brook, New York, USA. <sup>2</sup>Program in Neurosciences and Mental Health, Hospital for Sick Children, Toronto, Ontario, Canada. <sup>3</sup>Institute of Medical Science, University of Toronto, Toronto, Ontario, Canada. <sup>4</sup>Program in Neuroscience, SUNY at Stony Brook, Stony Brook, New York, USA. <sup>5</sup>Department of Physiology, University of Toronto, Toronto, Ontario, Canada. Correspondence should be addressed to S.G. (sge@notes.cc.sunysb.edu) or P.F. (paul.frankland@sickkids.ca).

Received 27 June; accepted 15 October; published online 11 November 2012; doi:10.1038/nn.3260

**Figure 1** Adult-born neurons form functional synapses on CA3 pyramidal neurons. **(a)** Top, experimental timeline. Bottom, image showing adult-born DGCs (4 wpi) and their axons (EGFP<sup>+</sup>). Scale bar represents 50  $\mu$ m. DG, dentate gyrus. **(b)** Light pulses (473 nm, 5 ms) elicited action potentials in Chr2-EGFP-infected, but not neighboring (EGFP<sup>-</sup>) DGCs. Left, image showing recorded DGCs filled with biocytin (white) in an acute brain slice (4 wpi). A Chr2-EGFP<sup>+</sup> newborn neuron (green and white) is shown in i, and a non-infected neighbor (white) is shown in ii. Scale bar represents 50  $\mu$ m. Right, light-induced action potentials in EGFP<sup>+</sup> (i), but not in EGFP<sup>-</sup> (ii) DGCs. **(c)** Optically evoked EPSCs from adult-born DGCs. Left, image showing Chr2-EGFP<sup>+</sup> axonal terminals (green) of adult-born DGCs (4 wpi) and a recorded CA3 pyramidal neuron (white). Scale bar represents 25  $\mu$ m. Right, a sample optically evoked EPSCs recorded from this cell, subsequently blocked by 50  $\mu$ M CNQX. **(d)** Axon integration (left, EGFP) and formation of functional synapses on CA3 neurons (right) at 1, 2, 3 and 4 wpi. Scale bar represents 10  $\mu$ m. **(e)** Amplitude of EPSCs at 1, 2, 3, 4, 6 and 8 wpi ( $P < 0.05$ ,  $n = 5$ –15 cells, two-tailed unpaired  $t$  test). **(f)** Latency of EPSCs at 2, 3, 4, 6 and 8 wpi. **(g)** Summary of EPSCs that were inhibited by 50  $\mu$ M L-AP4 ( $t = 5.465$ ,  $P = 0.012$ ,  $n = 5$  cells, two-tailed paired  $t$  test) or 1  $\mu$ M LY354740 ( $t = 3.891$ ,  $P = 0.027$ ,  $n = 6$  cells, two-tailed paired  $t$  test) and blocked by 50  $\mu$ M CNQX ( $t = 5.835$ ,  $P = 0.007$ ,  $n = 15$  cells, two-tailed paired  $t$  test). All values represent mean  $\pm$  s.e.m. \* $P < 0.05$ .



adult-born DGCs simultaneously to determine the development of functional output circuit in the CA3 area<sup>16,24</sup>. We constructed a retroviral vector expressing EGFP-tagged Channelrhodopsin 2 (Chr2-EGFP), a light-sensitive channel<sup>24,25</sup>, to birth date and specifically express Chr2-EGFP in adult-born hippocampal neurons<sup>10,11,16</sup>. Chr2-EGFP retroviruses were microinjected into the hilus of the dentate gyrus in adult mice and acute brain sections were prepared 1–8 weeks post infection (wpi)<sup>11</sup> (**Fig. 1a** and **Supplementary Fig. 1a,b**; see Online Methods). As expected, Chr2-EGFP retroviruses specifically targeted neural progenitors, and these cells gradually developed into typical DGCs (**Supplementary Fig. 1c–e**). Notably, brief pulses of blue light reliably induced action potentials in infected DGCs, but not in non-infected neighbors (**Fig. 1b**), indicating that this population of cells could be optically controlled. The infected cells were not illuminated during development and we did not observe changes in the intrinsic properties of newborn neurons expressing Chr2 at different ages than those expressing EGFP alone (**Supplementary Table 1**), which is consistent with previous findings where optogenes were expressed in other cell types<sup>24</sup>.

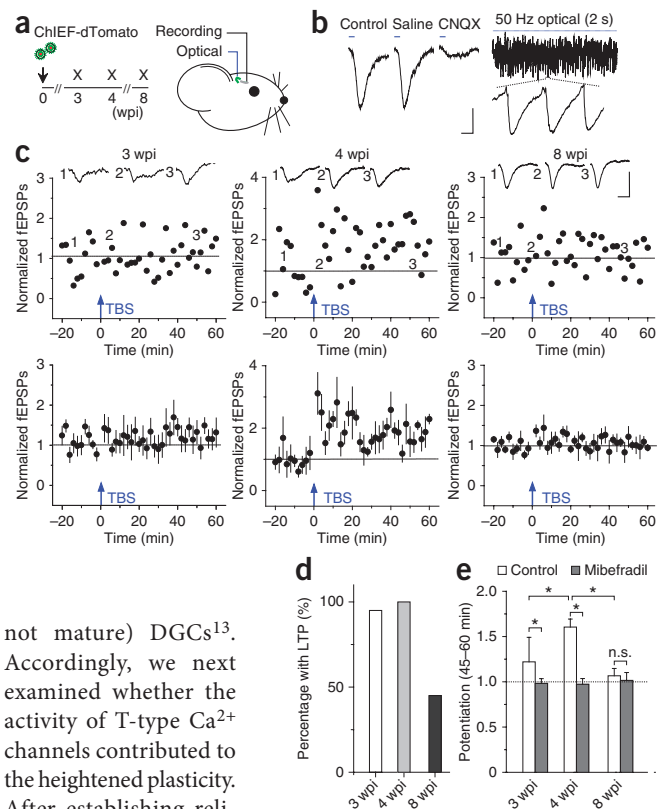
Next, we used whole-cell recording to examine postsynaptic currents in CA3 pyramidal neurons while optically stimulating Chr2-EGFP-positive mossy fibers of newborn DGCs (**Fig. 1c**). Postsynaptic activity increased with the age of infected adult-born DGCs (**Fig. 1d**). At 1 wpi, a time point at which mossy fibers have not yet reached the CA3 region, no postsynaptic responses were observed following optical stimulation. However, at 2 wpi and older (a stage at which mossy fibers have reached the CA3 region), stimulation produced excitatory

postsynaptic responses (EPSCs). These optically evoked EPSCs reached maximal responses at 4 wpi (**Fig. 1d,e**). They had a latency of ~4 ms and were blocked by an AMPA receptor antagonist (CNQX) and metabotropic glutamate receptor agonists (L-AP4 and LY354740, specifically blocking mossy fiber–CA3 synapses<sup>26</sup>), indicating that they represented a glutamatergic monosynaptic response (**Fig. 1f,g**). These results suggest that young adult-born DGCs form functional synapses with CA3 target cells, which become stable around 4 wpi. These findings, together with those of previous studies showing newborn neurons to be functionally innervated by entorhinal cortical projections<sup>10–12</sup>, indicate that adult-born DGCs fully integrate into the hippocampal trisynaptic circuits by ~4 wpi.

### Heightened synaptic plasticity of young adult-born neurons

We next characterized functional properties of these output synapses. We examined synaptic plasticity of young adult-born DGCs in the CA3 as previously described<sup>13,19</sup>. To optically stimulate CA3 synapses of a group of adult-born neurons at high frequency, we replaced the Chr2 construct with a Chr2 variant, ChIEF-dTomato<sup>27</sup>, which responds more reliably to high-frequency optical stimulation. As expected, 3-, 4- and 8-week-old adult-born DGCs expressing ChIEF responded reliably to theta-burst optical stimulation (TBS), a procedure used for long-term potentiation (LTP) induction<sup>13,19,27,28</sup> (**Supplementary Fig. 2a**), to their soma (**Supplementary Fig. 2b,c**). Recordings from axonal boutons revealed that, following optical stimulation, activation in soma could reliably propagate to the axonal terminals (**Supplementary Fig. 2d,e**), which is consistent with previous observations in mature

**Figure 2** Adult-born neurons at 4 weeks of age show enhanced plasticity at output synapses. **(a)** Experimental timeline. **(b)** Optically stimulating adult-born neurons produced fEPSPs in the CA3 area. Left, fEPSPs were blocked by infusion of 50  $\mu$ M CNQX (but not saline). Right, optical stimulation (50-Hz pulses of 5 ms) reliably induced fEPSPs. Scale bars represent 5 ms and 0.1 mV. **(c)** Theta-burst optical stimulation of adult-born neurons produced LTP at CA3 synapses in an age-dependent manner. Top, examples of fEPSPs LTP from a single animal at 3, 4 or 8 wpi. Insets, averaged traces of fEPSPs from five consecutive recordings before (1), immediately following (2) and after (3) LTP induction using TBS (blue arrow; **Supplementary Fig. 2**). Bottom, summary of LTP from groups of animals, respectively. **(d)** Percentage of mice (3, 4 and 8 wpi) exhibiting reliable LTP. **(e)** Summary of the mean potentiation of fEPSPs amplitude 45–60 min following TBS from mice under control condition (3, 4 and 8 wpi with 6, 8 and 8 animals, respectively; *t* test between groups: 3 versus 4 wpi, *t* = 3.386, *P* = 0.007; 8 versus 4 wpi, *t* = 4.483, *P* = 0.002) or after application of mibefradil (25 mg per kg, intraperitoneal; *t* test between control and mibefradil conditions: 3 wpi, *t* = 3.823, *P* = 0.007, *n* = 4; 4 wpi, *t* = 5.656, *P* < 0.001, *n* = 5; 8 wpi, *t* = 0.954, *P* = 0.41, *n* = 4). In each group, all animals tested with stable baseline were included. All values represent mean  $\pm$  s.e.m. n.s., not significant. *P* > 0.05, \**P* < 0.05, two-tailed unpaired *t* test.



DGCs<sup>29</sup>. To assess global circuit output of newborn neurons, we then implanted an optic fiber in the dentate gyrus to deliver optical stimulation and recorded field excitatory postsynaptic potentials (fEPSPs) in the CA3 region *in vivo* (**Fig. 2a** and **Supplementary Fig. 3**). fEPSPs were successfully induced by short pulses of optical stimulation (**Fig. 2b**). Similar to postsynaptic activity *in vitro* (**Fig. 1c**), fEPSPs recorded *in vivo* were blocked by local application of CNQX (**Fig. 2b**). As expected, high-frequency optical stimulation ( $\sim 5$  mW mm<sup>-2</sup> intensity, 50 Hz, 2 s) evoked consistent fEPSPs (**Fig. 2b**). Together with the reliable responses to TBS recorded from the soma or axonal terminals of newborn neurons (**Supplementary Fig. 2**), this result suggests that the experimental system is suitable for characterizing output synaptic plasticity of newborn DGCs using TBS. Thus, we next delivered TBS, and measured fEPSPs slope before and after TBS<sup>19</sup> (see Online Methods). We found that optical TBS at 3 and 4 wpi induced LTP of fEPSPs in the CA3 area in nearly all of the tested mice (**Fig. 2c,d**). When the same induction procedure was used to induce LTP at 8 wpi, only half of the tested mice exhibited potentiation (**Fig. 2c,d**). Thus, output synapses of adult-born DGCs at 4 wpi exhibit a lower induction threshold for LTP, similar to their input synapses<sup>13,19</sup>. We then analyzed LTP amplitude at 3, 4 and 8 wpi and found that LTP amplitude was maximal at 4 weeks. Relatively smaller LTP was observed in mice that were stimulated at 3 and 8 wpi (**Fig. 2c,e**). To determine whether the substantially reduced LTP at 8 wpi resulted from a lack of plasticity in the output synapses of newborn neurons around this age, we used a stronger induction procedure, tetanic optical stimulation (50 Hz, 2 s), for LTP induction while recording pyramidal cells (**Supplementary Fig. 4a**). Using this stronger induction protocol, we recorded sustained potentiation (**Supplementary Fig. 4b,c**), suggesting that the output synapses of mature newborn DGCs remain plastic, but have a higher induction threshold. However, using the same tetanic optical stimulation, we found a substantially higher level of LTP expression by stimulating young newborn neurons compared with that induced by stimulating mature newborn neurons (**Supplementary Fig. 4b–d**), consistent with our observation using theta-burst induction (**Fig. 2**). These results indicate that young newborn neurons exhibit heightened plasticity that peaks at  $\sim 4$  wpi (**Fig. 2e**).

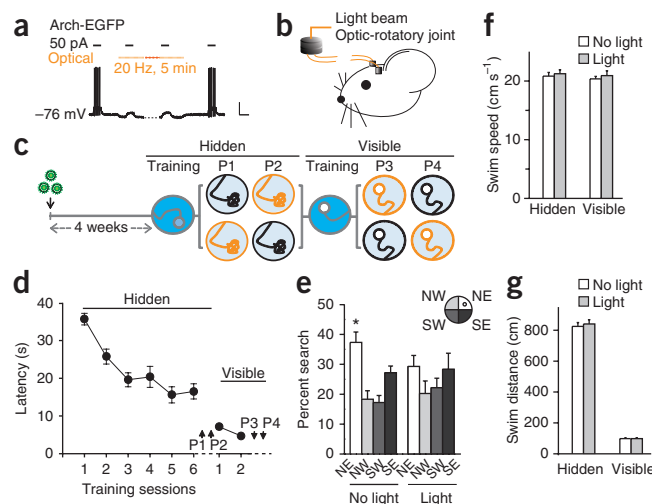
We next asked what might contribute to the heightened plasticity in young newborn neurons. A recent study found that T-type Ca<sup>2+</sup> channels facilitate dendritic synaptic plasticity in young newborn (but

not mature) DGCs<sup>13</sup>. Accordingly, we next examined whether the activity of T-type Ca<sup>2+</sup> channels contributed to the heightened plasticity. After establishing reliable recordings from the mice at 3, 4 and 8 wpi, we blocked T-type Ca<sup>2+</sup> channels with intraperitoneal injection of mibefradil (25 mg per kg of body weight), a specific T-type Ca<sup>2+</sup> channel blocker, and examined their role in the expression of output synaptic plasticity<sup>30</sup> (see Online Methods). Mibefradil showed no effect on the basal synaptic transmission (**Supplementary Fig. 5a,b**). Notably, optical TBS failed to induce an enhancement of synaptic transmission from mibefradil-treated mice at 3 and 4 wpi (**Fig. 2e**), at which point we observed robust potentiation in control animals using the same induction procedure (**Fig. 2e**). Although mibefradil is considered to be a specific blocker, it has been reported to block R-type Ca<sup>2+</sup> channels of some cultured cells at low dose<sup>31</sup>. To exclude this possibility, we performed recordings in hippocampal slices from mice at  $\sim 4$  wpi. Consistent with our *in vivo* data, application of mibefradil (1  $\mu$ M) abolished LTP of young DGCs, whereas SNX482 (500 nM), an R type-specific antagonist, failed to affect this LTP (**Supplementary Fig. 5c–f**). When mice were treated with mibefradil at  $\sim 8$  wpi, LTP seemed to be unaffected by the mibefradil application. Because of the small LTP expression using TBS at this age, we were unable to determine the effect precisely (**Fig. 2e**). However, together with previous observations of specific activation of T-type Ca<sup>2+</sup> channels in young neurons<sup>13</sup>, these data suggest that the activity of T-type Ca<sup>2+</sup> channels in young adult-born DGCs likely contributes to the heightened output synaptic LTP. Combined with previous studies on intrinsic excitability and input synapses<sup>13,19,32</sup>, these results reveal that a cohort of fully integrated ( $\sim 4$  weeks old) young newborn DGCs have more excitable membranes and enhanced input/output synaptic plasticity.

### Silencing young newborn neurons affects memory retrieval

Accumulating evidence suggests that the effectiveness of ablations of adult neurogenesis depend on the timing of manipulation<sup>2,5,7,8,23</sup>. This suggests that adult-born DGCs may assume distinct behavioral

**Figure 3** Reversibly silencing 4-week-old adult-born neurons impairs hippocampal memory retrieval. **(a)** Optical stimulation (589 nm) silences Arch-EGFP expressing adult-born neurons. Scale bars represent 100 ms and 30 mV. **(b)** Schematic drawing showing a mouse with implanted optrodes connected to an orange light source via optic fibers and an optic rotatory joint. **(c)** Timeline of water maze experiment. **(d)** Animals were trained with no light. Shown is the training curve of latency to find the platform. **(e)** Optically inactivating a cohort of 4-week-old adult-born neurons impaired hippocampal memory retrieval. During the probe, mice in the no light condition spent significantly more time searching in the target quadrant (NE) compared with the other quadrants (one-way repeated-measures ANOVA,  $F_{3,39} = 7.139$ ,  $P < 0.001$ ;  $NE > NW, SW$ , s.e.m. by paired  $t$  test planned comparison,  $n = 14$ ), showing robust spatial memory. In contrast, mice in the light condition (inactivation) didn't spend significantly more time in NE compared with the other quadrants ( $F_{3,39} = 0.9655$ ,  $P = 0.4187$ ;  $P > 0.05$  NE versus. NW, SW, SE;  $n = 14$ ), showing a disruption of spatial memory ( $NE_{no\ light} > NE_{light}$ ,  $t = 2.153$ ,  $P = 0.0253$  by planned comparison). **(f)** Optical inactivation did not alter swim speed in hidden probe tests (P1 and P2,  $t = 1.046$ ,  $P = 0.3145$ ,  $n = 14$ ) and visible probe tests (P3 and P4,  $t = 0.6464$ ,  $P = 0.2646$ ,  $n = 14$ ). **(g)** Optical inactivation did not alter swim distance in hidden probe tests (P1 and P2,  $t = 1.008$ ,  $P = 0.1660$ ,  $n = 14$ ) and visible probe tests (P3 and P4,  $t = 0.0173$ ,  $P = 0.09867$ ,  $n = 14$ ). All values represent mean  $\pm$  s.e.m. \* $P < 0.05$ , one-way ANOVA or two-tailed  $t$  test.



roles as they mature and that these distinct behavioral roles may coincide with changes in their synaptic integration and plasticity (Fig. 2e). To test this hypothesis, we used optogenetic stimulation to reversibly silence groups of different aged adult-born neurons during behavioral tasks. We generated a retrovirus to express an inhibitory optogene, archaerhodopsin-3 (Arch-EGFP)<sup>33</sup>. To maximize infection of adult-born neurons, we performed two retroviral injections (spaced 10 h apart) per mouse using a standard protocol<sup>11</sup> (see Online Methods). We successfully labeled  $\sim 1,700$  newborn DGCs per mouse at 4 wpi. Arch expression in labeled adult-born DGCs had no observable effect on the development of newborn neurons (Supplementary Table 1). In acutely prepared brain sections, pulses of optical stimulation specifically silenced Arch-expressing adult-born DGCs, indicating that the activity of these neurons could be reliably and reversibly inhibited by light (Fig. 3a), as previously reported<sup>33</sup>.

To examine the role of a group of newborn neurons in hippocampal memory, we used a hidden platform version of the water maze task<sup>34</sup>. We microinjected Arch-expressing retroviruses into the hilus of the hippocampus in adult mice and implanted customized optrodes to ensure sufficient light delivery into the dorsal hippocampus bilaterally (see Online Methods and Supplementary Fig. 6). At 4 wpi, mice were trained in the water maze with optic fibers connected to an orange light source via an optic-rotatory joint. Half of the mice were trained with the light off (no light group) and half with the light on (light group) (Fig. 3b and Supplementary Fig. 7a). Across the training trials, latencies to locate the hidden platform declined and there was no difference in escape latencies between control (no light) and inactivated (light) groups (Supplementary Fig. 7b), indicating that silencing this cohort of  $\sim 4$ -week-old adult-born DGCs does not interfere with memory acquisition.

We then assessed the effect of silencing newborn neurons on memory retrieval. At  $\sim 4$  wpi, mice were trained in the water maze with optic fibers connected to an inactive light source (no light), and the mice learned to locate the hidden platform (Fig. 3b–d). Following the completion of training, spatial memory was assessed in two probe tests. During the first probe, half of the animals received light stimulation for the duration of the test (light) and half were tested without the light (no light). On the following day, the animals were re-tested in a second probe trial with the light conditions reversed (Fig. 3c,d).

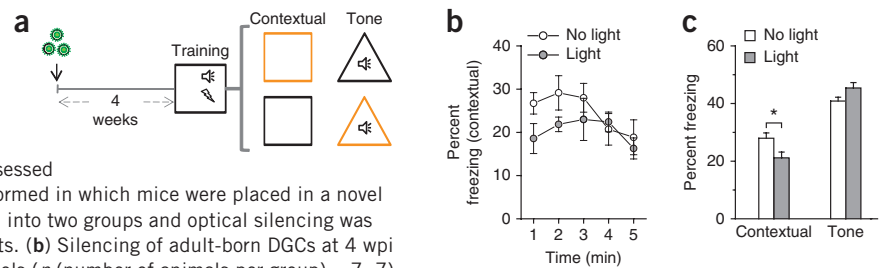
Using this within-subject design, we found that inactivation of this cohort of 4-week-old adult-born neurons robustly decreased the percentage of the time that the mice spent searching in the target quadrant (Fig. 3e). Notably, light illumination of 4-week-old EGFP-labeled newborn neurons did not affect the percent time in the target quadrant (Supplementary Fig. 8). Furthermore, light-induced inactivation did not affect motor coordination, as swim speed (Fig. 3f) and distance traveled (Fig. 3g) did not differ between the no light and light conditions. Memory impairments depended on both retroviral expression of Arch and light illumination, as neither retroviral expression of Arch alone (without illumination) nor illumination alone (in the absence of Arch) impaired memory<sup>10</sup> (Supplementary Fig. 8). These results suggest that a cohort of  $\sim 4$ -week-old newborn cells is important for memory expression. By examining expression of the activity-regulated gene, c-Fos, we next asked whether this population of cells was normally activated by memory recall and whether this activation was absent following light-induced inactivation. Mice received injections of Arch- or EGFP-expressing retrovirus into the dentate, and were trained in the water maze task 4 weeks later. At the completion of training, half of the mice were given a probe test with the light on and the other half with no light (Supplementary Fig. 9a). Using standard procedures<sup>21</sup>, 90 min after the probe tests, we killed the mice and performed c-Fos staining. We imaged c-Fos<sup>+</sup> and EGFP<sup>+</sup> Arch<sup>+</sup> DGCs (Supplementary Fig. 9b). Mice in the Arch and no light and EGFP groups searched selectively in the probe test, as expected. Following this probe test, we found that about 4% of labeled adult-born DGCs were c-Fos positive (Supplementary Fig. 9c), consistent with our previous findings<sup>21</sup>. In contrast, mice in the Arch and light group searched less selectively in the probe test (similar to deficits observed in Fig. 3d), and very few Arch-labeled adult-born DGCs expressed c-Fos (Supplementary Fig. 9b,c), confirming the efficiency of optical inhibition and providing support for the conclusion that labeled  $\sim 4$ -week-old adult-born DGCs regulate spatial memory retrieval.

We next evaluated whether silencing these neurons interfered with the expression of a non-hippocampus-dependent memory. The same mice were trained in a visible version of the water maze in which the platform was located in the opposite quadrant of the pool and marked by a visible cue. Across 2 d of training, mice learned to navigate to the cue from different start positions (Fig. 3c,d). During two subsequent

**Figure 4** Temporary silencing of 4-week-old newborn neurons impairs expression of a fear conditioning memory. **(a)** Timeline of fear conditioning test. Adult mice were infused with a retroviral vector (Arch-EGFP), implanted with optrodes and trained in fear conditioning (single tone-shock pairing). Contextual fear memory was assessed

24 h after training. An additional tone test was performed in which mice were placed in a novel context and the tone replayed. Animals were divided into two groups and optical silencing was counterbalanced in contextual and tone freezing tests. **(b)** Silencing of adult-born DGCs at 4 wpi reduced freezing to the context compared with controls ( $n$  (number of animals per group) = 7, 7).

**(c)** Optically inactivating adult-born DGCs at 4 wpi reduced freezing to the context (first 2 min of the context test,  $t = 2.239$ ,  $P = 0.0224$ ,  $n = 7, 7$ ), but had no effect on tone fear memory ( $t = 1.675$ ,  $P = 0.0599$ ,  $n = 7, 7$ ). To avoid potential interference from within session extinction, we measured freezing time in the first 2 min. All values represent mean  $\pm$  s.e.m. \* $P < 0.05$ , two-tailed  $t$  test.



probe tests, we found that light inactivation did not interfere with the latency of the mice to find the visible platform (no light,  $4.92 \pm 0.26$  s; light,  $4.87 \pm 0.34$  s;  $t = 0.1215$ ,  $P = 0.4526$ ,  $n = 14$ ; two-tailed unpaired  $t$  test), swimming (Fig. 3f) or distance traveled (Fig. 3g).

To ask whether our results would generalize to another form of hippocampus-dependent memory, we next trained a new group of animals in a fear-conditioning procedure<sup>35</sup> (Fig. 4a). Mice were trained with a single tone-shock pairing and tested in the same context 1 d later. In this test, optogenetic silencing reduced levels of conditioned freezing (Fig. 4b,c), indicating that inactivating 4-week-old adult-born neurons impairs the retrieval of contextual fear memory. The following day, we placed the mice in an alternate context and presented the tone. In contrast, optogenetically silencing these neurons did not affect conditioned freezing of the mice to the tone (Fig. 4c). As the retrieval of contextual, but not tone, fear memories depends on hippocampal function<sup>35</sup>, these results suggest that silencing a cohort of 4-week-old adult-born DGCs impairs retrieval of a hippocampus-dependent contextual fear memory.

### The behavioral role for newborn DGCs relies on their age

We next asked whether silencing different aged cohorts of newborn neurons would have a similar effect on hippocampal memory retrieval. To address this, we trained mice at 2 or 8 wpi. Silencing cells that were ~2-week-old at the time of training did not disrupt expression of spatial memory (Fig. 5a). Similarly, silencing cells that

were ~8 weeks old at the time of training, an age at which they are considered to be mature<sup>11,12,17</sup> (Fig. 1), did not affect expression of a spatial memory (Fig. 5b). Thus, silencing newborn neurons at ~4 wpi, but not at 2 or 8 wpi, resulted in deficits in spatial memory retrieval (Fig. 5c). Furthermore, silencing newborn neurons at 2 or 8 wpi did not affect contextual fear memory (Fig. 5d).

Not all adult-born DGCs survive, and the absence of effects of silencing at 8 weeks might be a result of there being fewer Arch<sup>+</sup> cells. Accordingly, we counted Arch<sup>+</sup> newborn DGCs after behavioral tests. We found that there was no obvious decrease in number of Arch-labeled neurons from 4 to 8 wpi (4 wpi,  $1,746 \pm 52$  labeled neurons per animal,  $n = 17$ ; 8 wpi,  $1,721 \pm 59$  labeled neurons per animal,  $n = 10$ ;  $P = 0.23$ , two-tailed unpaired  $t$  test), consistent with previous findings<sup>1,4,36</sup>. Furthermore, we found that Arch<sup>+</sup> cells had similar dendritic complexity ~4 and 8 wpi (4 wpi,  $9.85 \pm 1.08$  dendrites per  $50 \mu\text{m} \times 50 \mu\text{m}$ ,  $n = 17$ ; 8 wpi,  $10.27 \pm 0.95$  dendrites per  $50 \mu\text{m} \times 50 \mu\text{m}$ ,  $n = 10$ ;  $P = 0.78$ , two-tailed unpaired  $t$  test).

Finally, we asked whether the coincidentally heightened plasticity (Fig. 2) contributes to the role of young newborn neurons in retrieval of hippocampal-dependent memories. Given that we found that the activity of T-type Ca<sup>2+</sup> channels is essential for the heightened plasticity of output synapses, we tested hippocampal memory of the Arch-injected mice at 4 wpi with intraperitoneal administration of mibefradil (25 mg per kg). Notably, the application of mibefradil substantially decreased the searching time in the target quadrant

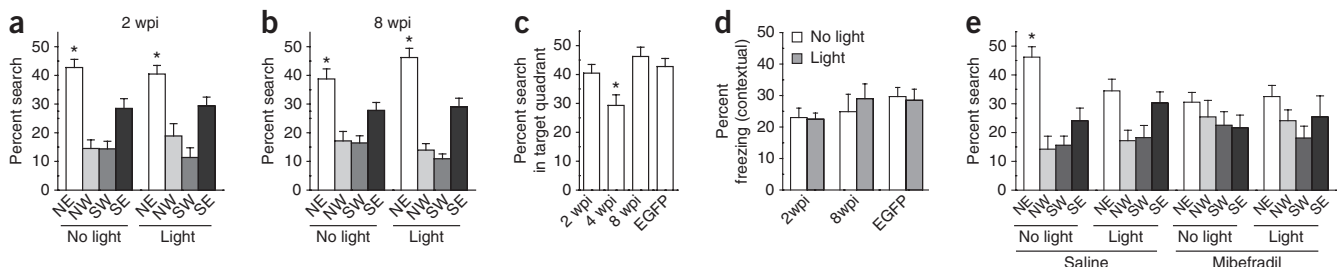
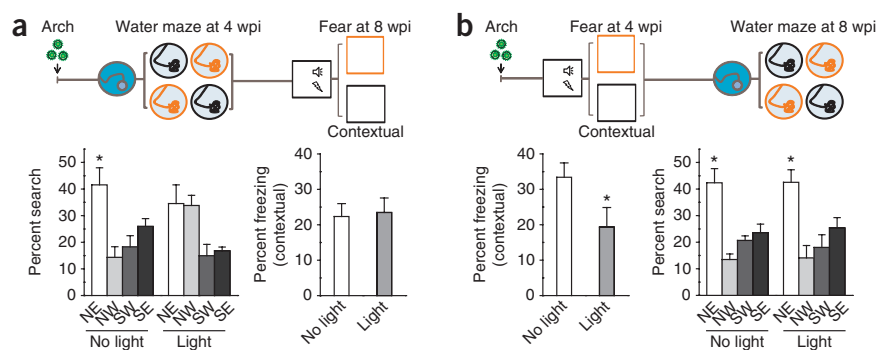


**Figure 5** Behavioral roles of adult-born DGCs are sensitive to their age. **(a,b)** Silencing adult-born DGCs at 2 or 8 wpi showed no significant effect on memory retrieval. Mice at 2 **(a)** or 8 **(b)** wpi spent more time searching in the target quadrant (NE) than the other quadrants in both no light (one-way repeated-measures ANOVA: 2 wpi,  $F_{3,15} = 15.25$ ,  $P < 0.0001$ ; 8 wpi,  $F_{3,15} = 8.081$ ,  $P = 0.0019$ ; NE > NW, SW, s.e.m. by paired  $t$  test planned comparison in both;  $n = 6, 6$ ) and light conditions (2 wpi,  $F_{3,15} = 9.125$ ,  $P = 0.0011$ ; 8 wpi,  $F_{3,15} = 14.20$ ,  $P = 0.0001$ ; NE > NW, SW, s.e.m. in both;  $n = 6, 6$ ). **(c)** Silencing adult-born DGCs affected memory retrieval in an age-dependent manner. The 4 wpi group showed significantly less time searching in the target quadrant in the light condition ( $n = 14$ ) compared with the 2 wpi ( $n = 6$ ,  $t = 2.360$ ,  $P = 0.030$ ), 8 wpi ( $n = 6$ ,  $t = 2.922$ ,  $P = 0.0135$ ), and EGFP 4 wpi ( $n = 8$ ,  $t = 2.392$ ,  $P = 0.0286$ ) groups by two-tailed unpaired  $t$  test. **(d)** Silencing of adult-born DGCs at 2 or 8 wpi failed to affect fear memory retrieval. Percent freezing of Arch animals at 2 wpi ( $t = 0.2029$ ,  $P = 0.4246$ ,  $n = 5$ ), 8 wpi ( $t = 0.3824$ ,  $P = 0.3568$ ,  $n = 8$ ) or EGFP at 4 wpi ( $t = 0.4593$ ,  $P = 0.3326$ ,  $n = 6$ ). Two-tailed paired  $t$  test comparison was made between no light and light conditions. **(e)** Mibefradil prevented hippocampal memory retrieval of the animals at 4 wpi. Shown is a summary similar to those in **a** (saline<sub>no light</sub>,  $F_{3,9} = 10.43$ ,  $P = 0.0027$ , NE > NW, SW, SE; saline<sub>light</sub>,  $F_{3,9} = 2.849$ ,  $P = 0.0975$ ; mibefradil<sub>no light</sub>,  $F_{3,9} = 1.173$ ,  $P = 0.3730$ ; mibefradil<sub>light</sub>,  $F_{3,9} = 1.061$ ,  $P = 0.4128$ ;  $n = 4, 4$  for all). All values represent mean  $\pm$  s.e.m. \* $P < 0.05$ ;  $n$  is the number of animals per group, one-way ANOVA or two-tailed  $t$  test.

**Figure 6** Task-switching experiments showing that adult-born DGCs at 4 wpi are important for memory retrieval. (a) Top, timeline of water maze and fear-conditioning tests. Bottom, at 4 wpi, water maze-trained animals under the no light condition searched selectively (ANOVA,  $F_{3,12} = 9.487$ ,  $P = 0.0017$ ; NE > NW, SW, SE;  $n = 5, 5$ ; see Figs. 3–5), whereas in the light condition they failed to search selectively ( $F_{3,12} = 4.004$ ,  $P = 0.0345$ ; NE versus NW,  $t = 0.0702$ ,  $P = 0.43$ ; NE versus SW,  $t = 1.792$ ,  $P = 0.077$ ). When trained in the contextual fear conditioning at 8 wpi, animals displayed a similar percent freezing ( $t = 0.3600$ ,  $P = 0.3685$ ). (b) Top, timeline of fear conditioning and water maze tests. Experiments were performed as described in a, but the order of behavioral tests was switched: fear condition and then water maze. Bottom, animals showed a significant decrease in percent freezing ( $t = 3.046$ ,  $P = 0.0191$ ) when trained at 4 wpi. However, at 8 wpi, both no light and light groups showed intact water maze memory (no light,  $F_{3,12} = 14.48$ ,  $P = 0.0003$ ; light,  $F_{3,12} = 9.644$ ,  $P = 0.0016$ ; NE > NW, SW, SE;  $n = 5, 5$ ). All values represent mean  $\pm$  s.e.m. \* $P < 0.05$ ,  $n$  is the number of animals per group, one-way ANOVA or two-tailed paired  $t$  test.



compared with the saline and no light groups (Fig. 5e). In another group of mice, in which we applied mibefradil and optical inhibition, we observed a similar deficit in memory retrieval in the mibefradil-treated mice (Fig. 5e). Because the activity of T-type  $\text{Ca}^{2+}$  channels is also required for the heightened plasticity in dendritic synapses<sup>13</sup>, these data suggest that heightened plasticity in young newborn neurons may be important for memory retrieval. To further explore the age specificity of these effects in the same cohort of newborn neurons, we designed a within-subject experiment in which mice were tested with the water maze at 4 wpi and contextual fear conditioning at 8 wpi, or vice versa (Fig. 6). We found that silencing newborn neurons at 4 wpi, but not 8 wpi, disrupted memory retrieval in both tasks, consistent with our observations (Figs. 3–5). Together, our data suggest that adult-born neurons may be transiently critical for memory retrieval, but the effect, at least in spatial and contextual memory retrieval, may decline as these adult-born neurons continue to mature.

## DISCUSSION

We used optogenetic methods to evaluate how adult-born DGCs functionally integrate into hippocampal circuits. We found that newborn DGCs form functional glutamatergic synapses in the CA3 area as early as 2 wpi and that these synapses become functionally stable by 4 wpi. The output synapses of 4-week-old newborn neurons exhibited enhanced plasticity. Notably, reversibly silencing a population of 4-week-old, but not 2- or 8-week-old, newborn DGCs affected hippocampal memory retrieval. These data indicate that adult-born neurons influence hippocampal function and behaviors in a maturation-dependent manner.

### Functional output circuit development

We successfully employed a retroviral method to deliver optogenes into cohorts of adult-born DGCs. As we previously reported<sup>10,11</sup>, infection with these retroviruses did not appear to affect the development of labeled newborn neurons (Supplementary Fig. 1 and Supplementary Table 1). By using optogenetic stimulation, physiology and imaging, we found that adult-born neurons functionally project to the CA3 neural circuitry. Blockade of postsynaptic responses by applying AMPA receptor antagonists or metabotropic glutamate receptor agonists revealed that they are typical mossy fiber synapses<sup>26</sup> (Fig. 1e). Together with several previous studies<sup>10–12,17</sup>, our results suggest that adult-born DGCs fully incorporate into the hippocampal trisynaptic neural circuit around 4 wpi.

We further found that output synapses of adult-born DGCs exhibited enhanced plasticity at ~4 wpi (Fig. 2). This mirrors the time during which we observed hyper-sensitive input synapses and during which these cells have more excitable membranes<sup>13,19</sup>. Mechanistically, we found that mibefradil, a T-type  $\text{Ca}^{2+}$  channel blocker, was able to abolish the heightened axonal plasticity of young newborn neurons, similar the effect it has on their dendritic synapses<sup>13</sup>. Although it is possible that mibefradil affects R-type  $\text{Ca}^{2+}$  channels<sup>31</sup>, heightened plasticity was not blocked by the application of SNX-482, an R-type  $\text{Ca}^{2+}$  channel antagonist. Considering previous studies showing its specificity<sup>30,37,38</sup> and young DGCs representing a hyperactive population with high-level T-type  $\text{Ca}^{2+}$  channels<sup>13</sup>, we think that T-type  $\text{Ca}^{2+}$  channels are very likely the major targets of mibefradil. In addition, the mechanisms described in the dendritic synapses of adult-born DGCS<sup>19,20,26,39</sup> may contribute to the heightened axonal plasticity<sup>40</sup>. Although the precise mechanisms remain to be determined, impaired spatial memory following blockade of T-type channels suggest that these channels have important functional roles in adult-born neurons.

### Time-dependent role of young adult-born neurons

Chemical, genetic and irradiation-based methods have been widely used to ablate neurogenesis and explore the role of adult neurogenesis in hippocampal function<sup>5,41</sup>. Although these studies have suggested that adult neurogenesis is important for hippocampal memory, they are limited in that these manipulations typically affect differently aged adult-born cells. Using retrovirally expressed optogenes, we were able to address this issue by labeling and silencing distinct cohorts of adult-born neurons. This optogenetic silencing of adult-born neurons by high-frequency light stimulation is likely to result from effective, but not excessive, hyperpolarization, rather than from potentially harmful changes in internal chloride levels<sup>33</sup>.

Our results suggest that silencing of ~4-week-old newborn neurons leads to memory deficits. In contrast, silencing this same population before training did not prevent the acquisition of a hippocampal memory. The dissociation is consistent with our recent findings using a transgenic diphtheria toxin-based ablation system to study the role of adult-born neurons in hippocampal memory<sup>7</sup> and suggests that learning may occur in the absence of newborn neurons. However, if newborn neurons are present and functional in circuit level at the time of training, they are recruited into hippocampal memory circuits, and silencing (or ablating<sup>7</sup>) these cells revealed that they are essential for memory retrieval. In our previous diphtheria toxin-based ablation study, adult-born cells spanning a range of ages (including

~4-week-old cells) were targeted<sup>7</sup>. Our finding that substantial memory retrieval deficits were only observed after silencing of ~4-week-old newborn neurons raises the possibility that the deficits following post-training ablation observed in our previous study were primarily driven by the loss of ~4-week-old newborn neurons. Still, we cannot exclude the possibility that silencing ~8-week-old newborn neurons also affects hippocampal function, albeit to a lesser degree. Finally, it is noteworthy that the retroviral approach only labeled a relatively small group of newborn neurons, and, thus, even the activity of this small population of cells strongly influenced hippocampal function. Although silencing a similar population before training did not impair memory acquisition, it is likely that silencing a larger population might induce anterograde memory deficits.

## METHODS

Methods and any associated references are available in the [online version of the paper](#).

Note: Supplementary information is available in the [online version of the paper](#).

## ACKNOWLEDGMENTS

We thank J. Bischofberger, G. Matthews, L. Role and H. Song for their critical comments, and Q. Xiong and J. Tucciarone for technical support. We thank the members of F. Gage's laboratory for sharing their behavioral protocols. This work was supported by US National Institutes of Health (NS065915), American Heart Association (0930067N), Feldstein Medical Foundation and State University of New York Research Excellence in Academic Health grants to S.G. and Canadian Institutes of Health Research grants to P.W.F. (MOP86762) and S.A.J. (MOP74650).

## AUTHOR CONTRIBUTIONS

Y.G. conducted all of the electrophysiological, immunohistochemical and confocal imaging analyses. Y.G. and M.A.-C. performed all of the behavioral analyses. J.W. engineered retroviral constructs and Y.G. produced retrovirus. S.R.J. helped with some initial manuscript preparation. S.G. and P.W.F. supervised the project. S.G., P.W.F., S.A.J., Y.G. and M.A.-C. wrote the manuscript. All of the authors read and discussed the manuscript.

## COMPETING FINANCIAL INTERESTS

The authors declare no competing financial interests.

Published online at <http://www.nature.com/doi/10.1038/nn.3260>.

Reprints and permissions information is available online at <http://www.nature.com/reprints/index.html>.

- Kempermann, G., Gast, D. & Gage, F.H. Neuroplasticity in old age: sustained fivefold induction of hippocampal neurogenesis by long-term environmental enrichment. *Ann. Neurol.* **52**, 135–143 (2002).
- Ming, G.L. & Song, H. Adult neurogenesis in the mammalian brain: significant answers and significant questions. *Neuron* **70**, 687–702 (2011).
- Cameron, H.A. & McKay, R.D. Adult neurogenesis produces a large pool of new granule cells in the dentate gyrus. *J. Comp. Neurol.* **435**, 406–417 (2001).
- Kim, W.R., Christian, K., Ming, G.L. & Song, H. Time-dependent involvement of adult-born dentate granule cells in behavior. *Behav. Brain Res.* **227**, 470–479 (2011).
- Aimone, J.B., Deng, W. & Gage, F.H. Resolving new memories: a critical look at the dentate gyrus, adult neurogenesis, and pattern separation. *Neuron* **70**, 589–596 (2011).
- Sahay, A. *et al.* Increasing adult hippocampal neurogenesis is sufficient to improve pattern separation. *Nature* **472**, 466–470 (2011).
- Arruda-Carvalho, M., Sakaguchi, M., Akers, K.G., Josselyn, S.A. & Frankland, P.W. Post-training ablation of adult-generated neurons degrades previously acquired memories. *J. Neurosci.* **31**, 15113–15127 (2011).
- Drew, M.R., Denny, C.A. & Hen, R. Arrest of adult hippocampal neurogenesis in mice impairs single- but not multiple-trial contextual fear conditioning. *Behav. Neurosci.* **124**, 446–454 (2010).
- Snyder, J.S., Soumier, A., Brewer, M., Pickel, J. & Cameron, H.A. Adult hippocampal neurogenesis buffers stress responses and depressive behavior. *Nature* **476**, 458–461 (2011).
- van Praag, H. *et al.* Functional neurogenesis in the adult hippocampus. *Nature* **415**, 1030–1034 (2002).
- Ge, S. *et al.* GABA regulates synaptic integration of newly generated neurons in the adult brain. *Nature* **439**, 589–593 (2006).
- Esposito, M.S. *et al.* Neuronal differentiation in the adult hippocampus recapitulates embryonic development. *J. Neurosci.* **25**, 10074–10086 (2005).
- Schmidt-Hieber, C., Jonas, P. & Bischofberger, J. Enhanced synaptic plasticity in newly generated granule cells of the adult hippocampus. *Nature* **429**, 184–187 (2004).
- Overstreet Wadiche, L., Bromberg, D.A., Bensen, A.L. & Westbrook, G.L. GABAergic signaling to newborn neurons in dentate gyrus. *J. Neurophysiol.* **94**, 4528–4532 (2005).
- Faulkner, R.L. *et al.* Development of hippocampal mossy fiber synaptic outputs by new neurons in the adult brain. *Proc. Natl. Acad. Sci. USA* **105**, 14157–14162 (2008).
- Toni, N. *et al.* Neurons born in the adult dentate gyrus form functional synapses with target cells. *Nat. Neurosci.* **11**, 901–907 (2008).
- Zhao, C., Teng, E.M., Summers, R.G. Jr., Ming, G.L. & Gage, F.H. Distinct morphological stages of dentate granule neuron maturation in the adult mouse hippocampus. *J. Neurosci.* **26**, 3–11 (2006).
- Hastings, N.B., Seth, M.I., Tanapat, P., Rydel, T.A. & Gould, E. Granule neurons generated during development extend divergent axon collaterals to hippocampal area CA3. *J. Comp. Neurol.* **452**, 324–333 (2002).
- Ge, S., Yang, C.H., Hsu, K.S., Ming, G.L. & Song, H. A critical period for enhanced synaptic plasticity in newly generated neurons of the adult brain. *Neuron* **54**, 559–566 (2007).
- Marin-Burgin, A., Mongiat, L.A., Pardi, M.B. & Schinder, A.F. Unique processing during a period of high excitation/inhibition balance in adult-born neurons. *Science* **335**, 1238–1242 (2012).
- Kee, N., Teixeira, C.M., Wang, A.H. & Frankland, P.W. Preferential incorporation of adult-generated granule cells into spatial memory networks in the dentate gyrus. *Nat. Neurosci.* **10**, 355–362 (2007).
- Tashiro, A., Makino, H. & Gage, F.H. Experience-specific functional modification of the dentate gyrus through adult neurogenesis: a critical period during an immature stage. *J. Neurosci.* **27**, 3252–3259 (2007).
- Nakashiba, T. *et al.* Young dentate granule cells mediate pattern separation, whereas old granule cells facilitate pattern completion. *Cell* **149**, 188–201 (2012).
- Zhang, F. *et al.* Multimodal fast optical interrogation of neural circuitry. *Nature* **446**, 633–639 (2007).
- Nagel, G. *et al.* Channelrhodopsin-2, a directly light-gated cation-selective membrane channel. *Proc. Natl. Acad. Sci. USA* **100**, 13940–13945 (2003).
- Nicoll, R.A. & Schmitz, D. Synaptic plasticity at hippocampal mossy fibre synapses. *Nat. Rev. Neurosci.* **6**, 863–876 (2005).
- Lin, J.Y., Lin, M.Z., Steinbach, P. & Tsien, R.Y. Characterization of engineered channelrhodopsin variants with improved properties and kinetics. *Biophys. J.* **96**, 1803–1814 (2009).
- Gunaydin, L.A. *et al.* Ultrafast optogenetic control. *Nat. Neurosci.* **13**, 387–392 (2010).
- Alle, H. & Geiger, J.R. Combined analog and action potential coding in hippocampal mossy fibers. *Science* **311**, 1290–1293 (2006).
- Yoshimura, Y. *et al.* Involvement of T-type Ca<sup>2+</sup> channels in the potentiation of synaptic and visual responses during the critical period in rat visual cortex. *Eur. J. Neurosci.* **28**, 730–743 (2008).
- Randall, A.D. & Tsien, R.W. Contrasting biophysical and pharmacological properties of T-type and R-type calcium channels. *Neuropharmacology* **36**, 879–893 (1997).
- Snyder, J.S., Kee, N. & Wojtowicz, J.M. Effects of adult neurogenesis on synaptic plasticity in the rat dentate gyrus. *J. Neurophysiol.* **85**, 2423–2431 (2001).
- Chow, B.Y. *et al.* High-performance genetically targetable optical neural silencing by light-driven proton pumps. *Nature* **463**, 98–102 (2010).
- Morris, R.G., Garrud, P., Rawlins, J.N. & O'Keefe, J. Place navigation impaired in rats with hippocampal lesions. *Nature* **297**, 681–683 (1982).
- Kim, J.J. & Fanselow, M.S. Modality-specific retrograde amnesia of fear. *Science* **256**, 675–677 (1992).
- Deng, W., Aimone, J.B. & Gage, F.H. New neurons and new memories: how does adult hippocampal neurogenesis affect learning and memory? *Nat. Rev. Neurosci.* **11**, 339–350 (2010).
- Bezprozvanny, I. & Tsien, R.W. Voltage-dependent blockade of diverse types of voltage-gated Ca<sup>2+</sup> channels expressed in *Xenopus* oocytes by the Ca<sup>2+</sup> channel antagonist mibefradil (Ro 40-5967). *Mol. Pharmacol.* **48**, 540–549 (1995).
- Bergquist, F. & Nissbrandt, H. Influence of R-type (Cav2.3) and T-type (Cav3.1–3.3) antagonists on nigral somatodendritic dopamine release measured by microdialysis. *Neuroscience* **120**, 757–764 (2003).
- Kerr, A.M. & Jonas, P. The two sides of hippocampal mossy fiber plasticity. *Neuron* **57**, 5–7 (2008).
- Ge, S., Sailor, K.A., Ming, G.L. & Song, H. Synaptic integration and plasticity of new neurons in the adult hippocampus. *J. Physiol. (Lond.)* **586**, 3759–3765 (2008).
- Sahay, A., Wilson, D.A. & Hen, R. Pattern separation: a common function for new neurons in hippocampus and olfactory bulb. *Neuron* **70**, 582–588 (2011).

## ONLINE METHODS

**Retroviral production and stereotaxic injection.** Engineered self-inactivating murine oncoretroviruses were used to deliver genes of interest specifically to proliferating cells and their progeny<sup>10,11</sup>. The optimized ChR2 constructs were obtained from K. Deisseroth (Stanford University) and the ChIEF construct from R. Tsien (Addgene). The Arch construct from E. Boyden was purchased from Addgene.

Purified engineered retroviruses were stereotaxically injected into adult C57BL/6 mice (Charles River). 5–6-week-old female mice were used for all experiments. For behavioral experiments, animals in each experimental group in general had slight different birth dates to minimize the potential effects from the estrous cycle. All mice were housed under standard conditions with 12-h:12-h dark/light cycle. All animal procedures were conducted in accordance with institutional guidelines and were approved by the Institutional Animal Care and Use Committee of Stony Brook University.

**Optrode implantation and behavioral procedures.** Optrodes (Doric Lenses, modified to increase light spread) were implanted bilaterally into the dorsal dentate gyrus (coordinates: 3.0 mm rostral from bregma, 2.6 mm lateral from the midline and 2.5 mm ventral) 14 d after two retroviral injections (~10-h interval) unless we specifically indicated otherwise in the main text. After implantation, animals received at least 2 weeks recovery before any behavioral experiment.

After behavioral experiments, mice were perfused transcardially with phosphate-buffered saline (PBS) followed by 4% (w/v) paraformaldehyde (PFA). Brains were sectioned and the optrode implantation sites were verified and numbers of retroviral-labeled adult-born neurons were counted. Mice were excluded if the implantation site was incorrectly positioned. Mice with missed viral injections were discarded. Mice with correct injections all had 1,500–2,000 newborn DGCS and all of them were selected for behavioral analysis.

**Water maze (hidden platform version).** The apparatus and behavioral procedures have been described previously<sup>21,42</sup>. Behavioral testing was conducted in a circular water maze tank (120 cm in diameter, 50 cm deep), located in a dimly lit room. The pool was filled to a depth of 40 cm with water made opaque by adding white, non-toxic paint. Water temperature was maintained at approximately 26 °C. A circular escape platform (10-cm diameter) was submerged 0.5 cm below the water surface, in a fixed position in one of the quadrants. The pool was surrounded by curtains, at least 1 m from the perimeter of the pool. The curtains were white with distinct cues painted on them.

Water maze training took place across 6 d. Each training session consisted of three training trials (inter-trial interval was ~15 s). On each trial, mice were placed into the pool, facing the wall, in one of four pseudorandomly varied start locations. The trial was complete once the mouse found the platform or 40 s had elapsed. If the mouse failed to find the platform on a given trial, it was guided onto the platform by the experimenter. Following training, spatial memory was assessed in two probe tests with the platform removed from the pool. The probe tests were 40 s in duration and conducted 24 h and 48 h after the last training session. Animals performed training and probes attached to the optic fibers and rotatory joint. Each animal experienced one probe with light stimulation and one without, the order of which was counterbalanced between animals. Behavioral data from training and the probe tests were acquired and analyzed using an automated tracking system (Ethovision XT, Noldus). Using this software, we recorded a number of parameters during training, including escape latency and swim speed. In probe tests, we measured the amount of time mice searched in the target quadrant versus the three other quadrants.

**Water maze (visible platform version).** For the visible platform task, the platform was moved to the opposite quadrant and marked by a visual cue. The cue consisted of a plastic cylinder (4 cm in diameter, 4 cm in height) with a horizontal black and white vertical-striped pattern and was placed on top of the platform. Visible platform training started 24 h after the last hidden platform probe and consisted of one training session of three trials per day (inter-trial interval was ~15 s) across 2 d. On each trial, mice were placed into the pool, facing the wall, in one of four start locations (pseudorandomly varied). The trial was complete once the mouse found the escape platform or 40 s had elapsed. Similar to the hidden version of the water maze, animals were divided into two groups to perform two probe tests, counterbalanced for order of light stimulation. The probes started 24 h after training and were

conducted on consecutive days. As before, behavioral data from training and the probe tests were acquired and analyzed using an automated tracking system.

**Context fear conditioning.** The fear conditioning chamber consisted of a stainless steel conditioning chamber (18 cm × 18 cm × 30 cm, Coulbourn) containing a stainless steel shock grid floor. Shock grid bars (diameter = 3.2 mm) were spaced 7.9 mm apart. The grid floor was positioned over a plastic drop-pan, which was lightly cleaned with 70% ethyl alcohol to provide a background odor. The front of the chamber was made of clear acrylic and the top, back and two sides made of modular aluminum. Animals were subjected to two probes, a context test and a tone test. For the context testing, animals were placed in the fear chamber, where they were originally shocked. For tone testing, mice were put in a modified version of the fear chamber that consisted of a white, plastic floor covering the shock grid bars and a plastic, triangular insert placed inside the same conditioning chamber used for training. One of the walls of this insert had a black- and white-striped pattern. The other two walls were white. After each test, the plastic floor was cleaned with water. Mouse freezing behavior was monitored via overhead cameras and scored manually.

During training, mice were placed in the fear conditioning chamber for a total of 3 min. After 2 min of free exploration mice were presented with a 30 s tone (2,800 Hz, 85 dB) that co-terminated with a 2-s foot shock (0.5 mA). Mice remained in the chamber for a further 30 s before being returned to their home cage.

We assessed freezing in two 5-min tests 24 h after training, in the fear chamber and its modified version, respectively. In the second probe, the tone was presented after a 2 min delay. Animals were divided into two groups for counterbalanced tests of the animals' freezing to the context and the tone, respectively. Data is presented as function of time for the context test. For the tone test, we measured freezing to the tone for 60 s.

**Slice and *in vivo* physiology.** Mice were processed at 1, 2, 3 and 4 wpi and electrophysiological recordings performed at 32–34 °C, as previously described<sup>11</sup>. For efferent CA3 synapse slice experiments, short pulses of blue light were generated by a 50-mW, 473-nm laser under the control of a standard digital converter board and launched into a Zeiss upright microscope through the epifluorescence light path. The ending power on brain slices was ~5 mW mm<sup>-2</sup> and synaptic transmission was recorded at -65 mV.

For *in vivo* recording, mice received injections of ChIEF-dTomato retrovirus 3, 4 and 8 weeks before *in vivo* recordings. Briefly, animals were anesthetized and mounted on a stereotaxic frame. An optrode was inserted into dorsal dentate gyrus (coordinates: 3.0 mm rostral from bregma, 2.6 mm lateral from the midline and 2.5 mm ventral). Pulses of blue light controlled by recording software (pClamp10.0) was generated from a 50-mW, 473-nm laser and delivered through an optic fiber. A recording electrode was inserted into CA3 molecular layer (coordinates: 2.0 mm rostral from bregma, 2.2 mm lateral from the midline and 2.2 mm ventral), and fEPSPs were recorded following optical stimulation of the dentate gyrus. After recording, mice were perfused transcardially with PBS followed by 4% PFA. Brains were sectioned to check for the presence of retroviral-labeled adult-born neurons and the sites of stimulation in dentate gyrus and recording in CA3 (Supplementary Fig. 3). Mice were excluded if the recording site was out of CA3. Slope of fEPSPs in each trace was measured and averaged every 2 min for analysis and plotting. For each animal, fEPSP slope values in the last 15 min (45–60 min) were compared with baseline values (-20–0 min) by two-tailed independent *t* test. Recording was considered a successful LTP if fEPSP slope values in the last 15 min were significantly greater than baseline (*P* < 0.05).

**c-Fos immunohistochemistry and analysis.** Neuronal activity during memory retrieval was analyzed by imaging immediate-early gene *c-Fos* expression as previously described<sup>24</sup> (Supplementary Fig. 9a). Briefly, 90 min following the completion of behavioral testing, mice were deeply anesthetized and perfused transcardially with PBS and then 4% PFA. Brains were removed, fixed overnight in PFA and then transferred to a 30% (w/v) sucrose solution and stored at 4 °C. Brains were sectioned into 50- $\mu$ m coronal sections covering the full anterior-posterior extent of the dentate gyrus. Immunohistochemistry was performed using primary antibody to *c-Fos* (rabbit polyclonal antibody, 1:1,000, Calbiochem, catalog no. PC38) and Alexa 568-conjugated goat antibody to rabbit (1:500, Molecular Probes, catalog no. A11011) as the secondary antibody. Sections were incubated in primary antibody overnight, and then with secondary antibody for 2 h at room temperature (25 °C), in the presence of 2% goat serum, 1% bovine



serum albumin and 0.2% (w/v) Triton X-100. Sections were mounted on slides with Permafluor anti-fade medium (Lipshaw Immunon). Images of the dentate gyrus were taken on an Olympus FLV1000 confocal microscope, and we quantified c-Fos<sup>+</sup> and EGFP<sup>+</sup> Arch<sup>+</sup> cells throughout the anterior-posterior extent of the granule cell layer. The numbers of c-Fos<sup>+</sup> cells and EGFP<sup>+</sup> Arch<sup>+</sup> cells were quantified from two-dimensional images of the entire dentate gyrus, and the ratio of c-Fos<sup>+</sup> to EGFP<sup>+</sup> Arch<sup>+</sup> cells was calculated for each animal.

**Staining and reconstruction of biocytin-filled neurons.** Brain sections with biocytin-filled neurons were fixed in 4% PFA overnight and stained using an Alexa 647-conjugated streptavidin from Invitrogen. Images were acquired on an Olympus FLV1000 confocal system and biocytin-filled neurons were reconstructed afterwards using Olympus FluoView10 software.

**Statistical analysis.** Data were analyzed using ANOVAs followed by *t* tests. Significance was considered to be  $P < 0.05$ . ANOVAs and most *t* tests are described in the figure captions. In the water maze, animals were considered to be searching selectively if the percent search in the northeast quadrant was significantly greater than that for each of the other quadrants (that is, northeast > northwest, northeast > southeast, and northeast > southwest). If the time spent in the northeast quadrant was not greater than that spent in all of the other quadrants, the search was considered to be not selective. For all behavioral experiments, animals were randomly grouped and data analysis was blinded. Cell counting and c-Fos analysis were performed blinded.

42. Teixeira, C.M., Pomedli, S.R., Maei, H.R., Kee, N. & Frankland, P.W. Involvement of the anterior cingulate cortex in the expression of remote spatial memory. *J. Neurosci.* **26**, 7555–7564 (2006).